Published in final edited form as:
Virology. 2009 June 5; 388(2): 335–343. doi:10.1016/j.virol.2009.03.030.

EBV BMRF-2 facilitates cell-to-cell spread of virus within polarized oral epithelial cells

Jianqiao Xiao[a], **Joel M. Palefsky**[a,b], **Rossana Herrera**[a], **Jennifer Berline**[a], and **Sharof M. Tugizov**[a,b,*]

[a]Department of Medicine, University of California, San Francisco, USA

[b]Department of Orofacial Sciences, University of California, San Francisco, USA

Abstract

We previously reported that the Epstein-Barr virus (EBV) BMRF-2 protein plays an important role in EBV infection of polarized oral epithelial cells by interacting with β1 and αv family integrins. Here we show that infection of polarized oral epithelial cells with B27-BMRF-2^{low} recombinant virus, expressing a low level of BMRF-2, resulted in significantly smaller plaques compared with infection by parental B95-8 virus. BMRF-2 localized in the trans-Golgi network (TGN) and basolateral sorting vesicles and was transported to the basolateral membranes of polarized epithelial cells. Mutation of the tyrosine- and dileucine-containing basolateral sorting signal, YLLV, in the cytoplasmic domain of BMRF-2 led to the failure of its accumulation in the TGN and its basolateral transport. These data show that BMRF-2 may play an important role in promoting the spread of EBV progeny virions through lateral membranes of oral epithelial cells.

Introduction

Epstein-Barr virus (EBV), a member of the human herpesvirus family, is the causative pathogen for infectious mononucleosis and is associated with several neoplastic diseases, including Burkitt's lymphoma, Hodgkins disease, and nasopharyngeal and gastric carcinomas (Rickinson and Kieff, 2001). EBV has tropism for B-lymphocytes and epithelial cells, where it causes latent and productive infection, respectively (Kieff and Rickinson, 2001).

The oropharyngeal mucosal epithelium is an important target for EBV infection, serving as a portal for viral entry in primary infection and the main site of release of progeny virions into saliva, thereby facilitating the spread of infectious virus within the human population. Productive EBV infection of the oropharyngeal epithelium has been shown in vivo (Greenspan and Greenspan, 1997; Greenspan et al., 1987; Greenspan et al., 1985; Lemon et al., 1977; Niedobitek et al., 1991; Rickinson, 1984; Sixbey et al., 1984; Young et al., 1988), ex vivo (Pegtel, Middeldorp, and Thorley-Lawson, 2004; Tugizov et al., 2007) and in vitro (Chang et al., 1999; Feederle et al., 2007; Sixbey et al., 1983; Tugizov, Berline, and Palefsky, 2003); however, the molecular mechanisms of EBV spread within the oral epithelium are not well understood.

*Corresponding Author: Sharof Tugizov, PhD, University of California, San Francisco, Department of Medicine, Box 0654, Phone: (415) 514-3177; Fax: (415) 476-9364; E-mail: sharof.tugizov@ucsf.edu.

The mechanisms of cell-to-cell spread of herpesviruses have been well investigated for alpha-herpesviruses, which have neuro-epithelial tropism and efficiently spread within neuronal and epithelial cell populations. Cell-to-cell spread of herpes simplex virus (HSV), varicella-zoster virus (VZV) and pseudorabies virus (PRV) occurs across the lateral junctions of epithelial cells, and a complex of two viral glycoproteins, gE and gI, plays a key role in this process (Alconada et al., 1998; Balan et al., 1994; Brack et al., 2000; Dingwell et al., 1994; Dingwell and Johnson, 1998; Johnson et al., 2001). The gE/gI complex first accumulates in the trans-Golgi network (TGN) and is then delivered to the cell junction area by basolateral sorting vesiscles (Farnsworth and Johnson, 2006; Johnson et al., 2001; McMillan and Johnson, 2001). The TGN localization and basolateral transport of gE/gI are facilitated by the interaction of clathrin adaptor complexes (eg., AP1, AP2, AP3 and AP4) with specific sorting signals in the cytoplasmic domains of these glycoproteins that contain tyrosine (YXXØ, where X is any amino acid and Ø is larger hydrophobic amino acid) and dileucine motifs and a cluster of acidic amino acids (Alconada et al., 1998; Alconada, Bauer, and Hoflack, 1996; Alconada, 1998; Dell'Angelica, Mullins, and Bonifacino, 1999; Folsch, 2005; Folsch et al., 1999; Folsch et al., 2003; Folsch et al., 2001; Ohno et al., 1995; Ohno et al., 1999; Renold et al., 2000; Simmen et al., 2002; Tirabassi and Enquist, 1998; Tirabassi and Enquist, 1999). The basolateral sorting signal of gE/gI leads to the accumulation of nascent virions at cell junctions and their spread via neighboring membranes (Farnsworth and Johnson, 2006; Johnson et al., 2001; McMillan and Johnson, 2001; Polcicova et al., 2005).

EBV and other gamma-herpesviruses lack genetic homologues of alpha-herpesvirus gE and gI; however, recent work on murine gamma-herpesvirus-68 (MHV-68) has shown that the MHV-68 glycoproteins gp48 and ORF58 play critical roles in cell-to-cell spread of virus (May et al., 2005a; May et al., 2005b). ORF58 forms a complex with gp48, facilitating its transport to the plasma membrane. The gp48/ORF58 protein complex induces plasma membrane projections that lead to the formation of intercellular contacts between infected and uninfected cells, enabling cell-to-cell spread of progeny virions (Gill et al., 2008). gp48 and ORF58 homologues are present in other gamma-herpesviruses, including EBV. Their homologues in EBV are the BDLF-2 and BMRF- proteins. It has recently been shown that EBV BDLF-2 and BMRF-2 also form a protein complex and that BMRF-2 facilitates the translocation of BDLF-2 to the cell surface (Gore and Hutt-Fletcher, 2008).

BMRF-2 is a transmembrane glycoprotein, and its major extracellular loop contains an Arg-Gly-Asp (RGD) motif, which interacts with the β1- and αv-family integrins of oral epithelial cells (Xiao et al., 2007). The BMRF-2–integrin interaction facilitates EBV infection of polarized oral epithelial cells through their basolateral membranes (Tugizov, Berline, and Palefsky, 2003; Xiao et al., 2008). BMRF-2 is highly expressed in a benign lesion of the oral epithelium known as hairy leukoplakia (HL) (Xiao et al., 2007), which occurs primarily in persons with HIV-associated immunodeficiency (Greenspan and Greenspan, 1997; Greenspan et al., 1987; Greenspan et al., 1985). BMRF-2 is transported to the basolateral membranes of both HL epithelial cells and EBV-infected polarized oral epithelial cells (Tugizov, Berline, and Palefsky, 2003; Xiao et al., 2007). The cytoplasmic tail of BMRF-2 contains a potential basolateral sorting signal with the sequence YLLV (aa 349–352), which includes both tyrosine and dileucine.

In this study we have investigated the role of EBV BMRF-2 in cell-to-cell spread of progeny virions in oral epithelial cells. We found that cell-to-cell spread of a recombinant EBV B27-BMRF-2^{low}, which expresses a low level of BMRF-2, is substantially reduced in comparison to that of parental EBV B95-8 virus. BMRF-2 was found to accumulate in the TGN and to be transported to the basolateral membranes through interaction with the μ subunits of the AP-4 basolateral sorting determinant. Mutation of the YLLV motif in the BMRF-2 cytoplasmic domain abolished BMRF-2 accumulation in the TGN, its colocalization with AP4-associated

vesicles and its transport to basolateral membranes of epithelial cells. These results suggest that EBV BMRF-2 may play an important role in sorting of intracellular progeny virions to the basolateral membranes of epithelial cells and spread of virus from infected to uninfected cells via their lateral membranes.

Results

The BMRF-2 protein may play an important role in efficient cell-to-cell spread of EBV in polarized oral epithelial cells

Previously we showed that EBV cell-to-cell spread may occur in polarized oral epithelial cells (Tugizov, Berline, and Palefsky, 2003) and that BMRF-2 was transported to the basolateral membranes of HL and EBV-infected polarized oral epithelial cells (Xiao et al., 2007), suggesting that BMRF-2 may be involved in EBV spread within the oral epithelium. To determine the role of BMRF-2 in cell-to-cell spread of viral progeny, we used recombinant B27-BMRF-2^{low} virus, which expresses only a low level of BMRF-2 protein (Xiao et al., 2008). To examine the susceptibility of polarized tongue and tonsil epithelial cells to EBV infection, cells were infected with parental B95-8 and recombinant B27-BMRF-2^{low} virus. Polarized cells were infected from their basolateral membranes at 100 virions/cell and analyzed at 3 days postinfection. Confocal immunofluorescence analysis of gp350/220 expression (data not shown) in two tongue and three tonsil epithelial cell lines infected with B95-8 showed that 8–12% of cells were infected with EBV. In contrast, only 2–3% of tongue and tonsil cells infected with B27-BMRF-2^{low} were positive for gp350/220, indicating that the number of cells infected with virus expression low level of BMRF-2 was 4–5 fold lower than that of cells infected with parental B95-8 virus.

To determine the role of BMRF-2 in cell-to-cell spread of virus, polarized tongue and tonsil epithelial cells were infected with B95-8 and B27-BMRF-2^{low} viruses at 0.3 virion/cell, resulting in infection of approximately 100 and 25 infected cells per Transwell insert (about 2×10^5 cells), respectively. Plaque development was evaluated in infected cells maintained for 3 weeks. To detect plaques generated by parental B95-8 virus, infected cells were immunostained for gp350/220 (Fig. 1A, upper panels). The average size of parental B95-8 -generated gp350/220-positive plaques was about 35 cells. The plaques generated by B27-BMRF-2^{low} virus were identified by gp350/220 staining and detection of GFP (Fig. 1A, lower panels), which is expressed only by the BMRF-2 knockout B27-BMRF-20 virus (Xiao et al., 2008). The average size of gp350/220- and GFP-positive B27-BMRF-2^{low} virus -generated plaques was about 6 cells (Fig. 1B), which was about 6-fold smaller then those generated by parental B95-8 virus. We did not observe significant variation in the size of plaques generated by B95-8 and B27-BMRF- 2^{low} viruses among tongue and tonsil cells derived from different donors.

We previously reported that the recombinant B27-BMRF-2^{low} viral population consists of about 85–90% BMRF-2 knockout recombinant viral episomes and 10–15% parental B95-8 viral episomes, which may lead to the generation of two viral subpopulations (Xiao et al., 2008). Therefore, we expected that some B95-8 virus-generated BMRF-2–positive larger plaques would appear in the epithelial cells infected with B27-BMRF-2^{low} virus. To distinguish between the two types of plaque, we examined BMRF-2 expression in B27-BMRF-2^{low} –infected cells by immunofluorescence assay using a rat anti-BMRF-2 serum. We found that the small, GFP-positive plaques (≈ 6 cells per plaque) were BMRF-2 negative (Fig. 2A, upper panel). In contrast, the large, GFP-negative plaques (≈ 30 cells per plaque) were strongly positive for BMRF-2 (Fig. 2A, lower panel). These data also were confirmed by co-immunostaining of B27-BMRF-2^{low} –infected cells for BMRF-2 (red) and gp350/220 (blue) (Fig. 2B). Confocal analysis showed that GFP-positive small plaques were negative for BMRF-2 and strongly positive for gp350/220 (Fig. 2B, white arrow) and that GFP-negative

large plaques were positive for BMRF-2 and gp350/220 (Fig. 2B, red arrow). These results indicate that GFP-positive and BMRF-2-negative small plaques were generated by BMRF-2 knockout virions and that GFP-negative and BMRF-2-positive large plaques were infected by parental B95-8 virus. Absence of BMRF-2 expression in GFP-positive small plaques suggest that this protein plays a key role in plague development, i.e., it may facilitate cell-to-cell spread of EBV in polarized oral epithelial cells.

The cytoplasmic tyrosine/di-leucine (YLLV) motif of BMRF-2 is essential for its surface transport in oral epithelial cells

Data from the above experiments suggest that EBV BMRF-2 may play a critical role in cell-to-cell spread of virus in polarized oral epithelial cells. Our previous work showed that in EBV-infected polarized oral epithelial cells, BMRF-2 was transported to the basolateral membranes (Xiao et al., 2007), consistent with its role in facilitating the spread of progeny virions via the lateral membranes of epithelial cells. Analysis of the BMRF-2 amino acid sequence revealed that amino acids 349 and 352 in its cytoplasmic tail constitute a tyrosine/dileucine YLLV motif (Fig. 3A), which may serve as a tyrosine/dileucine–based basolateral sorting signal in polarized epithelial cells. To determine the role of this potential sorting signal in BMRF-2 basolateral transport, we created site-specific mutants lacking the Y_{349} or $LL_{350–351}$ amino acids. To disrupt the function this motif, we replaced Y^{349} with A_{349} (BMRF-2_{YA}), and $LL_{350–351}$ with $GG_{350–351}$ (BMRF-$2_{LL\text{-}GG}$) (Fig. 3A). To study the functional role of these mutations in BMRF-2 transport we generated HSC-3^{sort} cell lines constitutively expressing GFP-tagged wt and mutant BMRF-2 proteins, designated HSC-BMRF-2_{wt}, HSC-BMRF-$2_{Y\text{-}A}$ and HSC-BMRF-$2_{LL\text{-}GG}$, respectively. Expression of wt and mutant BMRF-2 proteins in these cell lines was confirmed by Western blot assay (Fig. 3B).

To determine whether the Y_{349} or $LL_{350–351}$ residues in the YLLV motif are involved in BMRF-2 protein transport to the cell surface, we performed flow cytometry analysis of the HSC-BMRF-2_{WT}, HSC-BMRF-$2_{Y\text{-}A}$ and HSC-BMRF-$2_{LL\text{-}GG}$ cell lines. As shown in Fig. 4, the wt BMRF-2 protein was found to be highly expressed on the cell surface of HSC-BMRF-2_{wt} cells; however, the surface transport of BMRF-$2_{Y\text{-}A}$ and BMRF-$2_{LL\text{-}GG}$ mutant proteins was decreased by approximately 75% and 60%, respectively. These data clearly indicate that substitution of the tyrosine and di-leucine residues in the YLLV motif substantially reduces the transport of BMRF-2 to the cell surface of non-polarized oral epithelial cells.

Basolateral transport of BMRF-2 is mediated by its tyrosine/di-leucine (YLLV) sorting signals

To determine the role of the BMRF-2 cytoplasmic tyrosine/dileucine-containing YLLV motif in its basolateral sorting in polarized epithelial cells, we grew the HSC-BMRF-2_{WT}, HSC-BMRF-$2_{Y\text{-}A}$ and HSC-BMRF-$2_{LL\text{-}GG}$ cell lines under polarizing conditions. Expression of wt and mutant BMRF-2 proteins on the apical and basolateral membranes of epithelial cells was examined by a domain- specific labeling assay. In the HSC-BMRF-2_{WT} cell line about 10% of BMRF-2 was detected on the apical surface of the polarized cells, with the vast majority (about 90%) being detected on the basolateral membranes (Fig. 5). Domain-specific labeling of polarized HSC-BMRF-$2_{Y\text{-}A}$ and HSCBMRF-$2_{LL\text{-}GG}$ cells showed that both BMRF-$2_{Y\text{-}A}$ and BMRF-$2_{LL\text{-}GG}$ mutant proteins were present in both the apical and basolateral membranes at low levels, indicating non-polarized transport of these mutant proteins.

To confirm the finding that only the wt protein undergoes significant basolateral transport, we immunostained polarized HSC-BMRF-2_{WT}, HSC-BMRF-$2_{Y\text{-}A}$ and HSCBMRF- $2_{LL\text{-}GG}$ cells with a mouse mAb to pan-cadherin, a marker of the basolateral membranes of epithelial cells (Fig. 6). BMRF-2 expression was evaluated by detection of GFP. The development of a yellow signal in merge panels of both horizontal and vertical planes indicates the colocalization of BMRF-2 (green GFP signal) and pancadherin, immunolabeled with a red fluorescence signal.

We found that only wt BMRF- colocalized with the pan-cadherin (Fig. 6A). In contrast, the tyrosine (Fig. 6B) and dileucine mutants (Fig. 6C) did not colocalize with the basolateral marker. Together, these experiments show that mutation of either Y_{349} or $LL_{350–351}$ disrupts BMRF-2 transport to the basolateral membranes of polarized oral epithelial cells.

The BMRF-2 tyrosine/dileucine (YLLV) sorting signal mediates BMRF-2 accumulation in the TGN and the basolateral sorting compartment

Tyrosine/dileucine–mediated basolateral transport of cellular and viral membrane proteins has been shown to occur through the TGN and basolateral endosomic sorting compartments (Bonifacino et al., 1996; Bonifacino and Traub, 2003). To determine whether the BMRF-2 tyrosine/dileucine (YLLV) motif mediates BMRF-2 transport via the same pathway, we first examined localization of wt BMRF-2 and its tyrosine and dileucine mutants in the Golgi by co-staining of polarized HSC-BMRF-2_{WT}, HSCBMRF-$2_{Y\text{-}A}$ and HSC-BMRF-$2_{LL\text{-}GG}$ cells with the Golgi marker Rhodamine-Lens Culinaris Agglutinin. These data showed that wt BMRF-2 (Fig. 7, upper panel) and the mutant proteins lacking tyrosine (Fig. 7, lower panel) and dileucine (data not shown) motifs all colocalized with the Golgi marker. Next, we co-immunostained the polarized HSC-BMRF-2_{WT}, HSC-BMRF-$2_{Y\text{-}A}$ (Fig. 8) and HSC-BMRF-$2_{LL\text{-}GG}$ (data not shown) cell lines with antibodies to TGN46 and AP-4μ, which are markers for the TGN and basolateral sorting endosomes, respectively (Aguilar et al., 2001; Bonifacino et al., 1996; Bonifacino and Traub, 2003). Confocal microscopy revealed that wt BMRF-2 protein was strongly colocalized with both TGN46 (Fig. 8A, upper panels) and AP-4μ (Fig. 8B, upper panels), as indicated by the yellow signal in the merged panels. These results demonstrate wt BMRF-2 accumulation within the TGN and basolateral sorting endosomal compartments. In contrast, tyrosine (Fig. 8A and B, lower panels) and dileucine (data not shown) mutants of BMRF-2 only partially colocalized with TGN46 (Fig. 8A, lower panels) and AP-4μ (Fig. 8B, lower panels).

These findings indicate that BMRF-2 mutant proteins were transported from the endoplasmic reticulum (ER) to the Golgi, but did not enter significantly into the TGN and basolateral sorting compartments, which is consistent with a disruption of basolateral transport of these mutant proteins in polarized HSC-3 cells (Fig. 6B and C). Our results show that the Y_{349} and $LL_{350–351}$ residues in the YLLV motif of BMRF-2 are critical for accumulation of BMRF-2 in the TGN and entry into the basolateral sorting vesicles that mediate delivery to the basolateral membranes of oral epithelial cells.

Lack of BMRF-2 sorting to the basolateral membranes of polarized cells disrupts its interaction with integrins

We previously reported that wt BMRF-2 protein co-localizes with β1 integrin at the basolateral membranes of EBV-infected, polarized pharyngeal epithelial cells (Xiao et al., 2007). To confirm this finding in polarized cells expressing only the BMRF-2 protein in the absence of other viral proteins, we examined colocalization of wt BMRF-2 and its BMRF-$2_{Y\text{-}A}$ and BMRF-$2_{LL\text{-}GG}$ mutants with β1 and αv integrins. Immunolocalization experiments using mAbs to β1 and αv integrins were analyzed by laser confocal microscopy in both horizontal and vertical planes (Fig. 9). We found that wt BMRF-2 colocalized with β1 (Fig. 9A) and αv (data not shown) integrins. In contrast, both BMRF-$2_{Y\text{-}A}$ (Fig. 9B) and BMRF-$2_{LL\text{-}GG}$ (Fig. 9C) mutant proteins failed to colocalize with β1 and αv (data not shown) integrins, demonstrating that basolateral transport of BMRF-2 is important for its interaction with integrins.

Discussion

Accumulating evidence indicates that direct cell-to-cell transfer within epithelial, neuronal and other tissues is an efficient route for viral movement from infected to uninfected cells

(Sattentau, 2008). In epithelial tissues viral spread occurs mainly at or near cell junctions, where the membranes of adjacent cells are in close contact (Johnson and Huber, 2002; Sattentau, 2008). The presence of viral receptors within the cell-contact area facilitates the rapid spread of virus from infected to uninfected cells. The presence of extensive cell junctions (desmosomes and both tight and adherens junctions) may prevent penetration of neutralizing antibodies into these cell-to-cell contact areas and therefore protect the infectious virions from host immune surveillance (Johnson and Huber, 2002; Sattentau, 2008).

Previously we reported that EBV infection of oral explants *ex vivo* leads to the development of plaque-like foci that increase in size in a time-dependent fashion (Tugizov et al., 2007), suggesting that EBV dissemination within the oral epithelium may occur by direct spread of progeny virions from infected to uninfected epithelial cells. Plaque formation of EBV-infected epithelial cells in the presence of EBV-neutralizing sera indicated that cell-to-cell spread of progeny virions occurs within tightly connected lateral membranes, where antibody accessibility is restricted (Tugizov, Berline, and Palefsky, 2003).

Transport of BMRF-2 to the lateral membranes of HL epithelia and EBV-infected, polarized oral epithelial cells (Xiao et al., 2007) suggests that this protein plays an important role in cell-to-cell spread of progeny virions across the lateral membranes of epithelial cells. Therefore, in this study we investigated the role of BMRF-2 in cell-to-cell spread of EBV in primary oral epithelial cells, which are permissive for lytic EBV infection (Feederle et al., 2007; Pegtel, Middeldorp, and Thorley-Lawson, 2004; Tugizov, Berline, and Palefsky, 2003; Xiao et al., 2007).

Analysis of plaque development in tongue and tonsil epithelia infected with either the parental B95-8 EBV strain or the recombinant B27-BMRF-2^{low} strain revealed that the rate of cell-to-cell spread of the mutant virus was substantially lower than that of the parental virus. We previously reported that the B27-BMRF-2^{low} viral population consists predominantly of BMRF-2 knockout virions (85–90%) (Xiao et al., 2008), although it also contains a small percentage of parental virus. Therefore, it is possible that the presence of wt B95-8 virus in the B27-BMRF-2^{low} viral population may lead to the formation of plaques infected with both wt and BMRF-2 knockout viruses. However, our plaque formation assay for B27-BMRF-2^{low} virus was initiated with about 25 infected cells within the polarized monolayer (2×10^5 cells), which covers about 1 cm^2 of filter insert. It is unlikely that plaques infected with both the BMRF-2 knockout virus and the parental B95-8 virus would occur at the low infection density used in our experiments. Indeed, we were able to detect GFP-positive and BMRF-2-negative small plaques in the B27-BMRF-2^{low} virus-infected epithelial cells, indicating that these plaques were generated by the BMRF-2 knockout virus and not by the B95-8 parental virus. Development of small BMRF-2 negative plaques (about 5–6 cells) with BMRF-2 knockout virions is consistent with an important functional role for BMRF-2 in the cell-to- cell spread of EBV.

We have shown that the interaction of BMRF-2 with β1 (α5 β1 and α3 β1) and αv (αvβ3 and αvβ5) family integrins through its RGD domain is important for EBV infection of polarized oral epithelial cells (Tugizov, Berline, and Palefsky, 2003; Xiao et al., 2008; Xiao et al., 2007). EBV spread in the presence of EBV-neutralizing sera may occur only via lateral membranes of polarized epithelial cells, and given that integrins are present in the lateral membranes (Henning et al., 1994; Marchisio et al., 1991; Philp and Nachmias, 1987; Tugizov, Berline, and Palefsky, 2003), the BMRF-2-integrin interaction might facilitate direct spread of viral progeny from infected to adjacent, uninfected cells. Thus, the role of BMRF-2 in EBV infection of oral epithelial cells may occur in two distinct stages. In the first stage, BMRF-2 binding to integrins at the basal membranes of polarized cells promotes initial viral infection of polarized epithelial cells. In the second stage, BMRF-2 interaction with integrins at the

lateral membranes of epithelial cells facilitates the spread of progeny virions to adjacent, uninfected cells.

Herpes viruses acquire a final envelope in the sorting compartments of the TGN or the endosomes, where viral glycoproteins accumulate (Brack et al., 2000; Browne et al., 1996; Farnsworth, Goldsmith, and Johnson, 2003; Farnsworth, Wisner, and Johnson, 2007; Gershon et al., 1994; Skepper et al., 2001; Turcotte, Letellier, and Lippe, 2005; Whiteley et al., 1999; Zhu et al., 1996). Viral glycoproteins containing basolateral sorting signals may determine the sorting of nascent virions from the TGN to the basolateral membranes of epithelial cells. This model has been well established for alpha-herpesvirus spread in polarized epithelial cells, where the basolateral sorting signal of glycoproteins gE/gI plays a critical role in delivering the progeny virions to the lateral membranes (Alconada et al., 1998; Balan et al., 1994; Brack et al., 2000; Dingwell et al., 1994; Dingwell and Johnson, 1998; Farnsworth and Johnson, 2006; Johnson et al., 2001; McMillan and Johnson, 2001; Polcicova et al., 2005).

Less is known about intracellular sorting of nascent EBV virions in polarized epithelial cells. The identification of tyrosine- and dileucine-based basolateral sorting signals in the cytoplasmic tail of BMRF-2 suggests that this protein may be involved in lateral sorting of EBV progeny virions in polarized epithelial cells. Mutation of both the tyrosine and dileucine residues in the cytoplasmic YLLV motif of BMRF-2 did not reduce protein transport from the ER to the Golgi, but did abolish its accumulation in the TGN and its entry into AP-4μ-containing vesicles, resulting in the impaired transport of BMRF-2 to the lateral membranes of polarized epithelial cells. It has been shown that tyrosine- and dileucine-containing sorting signals may regulate transport of proteins from the biosynthetic compartments of polarized epithelial cells (ER/Golgi) to their TGN/endosomal sorting compartments and basolateral membranes (Aguilar et al., 2001; Hunziker et al., 1991; Rajasekaran et al., 1994; Sevier et al., 2000). Basolateral sorting of BMRF-2 in polarized oral epithelial cells is consistent with the reduced cell-to-cell spread of the recombinant EBV B27-BMRF-2^{low} virus that contain a low level of BMRF-2. However, we cannot exclude involvement in cell-to-cell spread by other EBV proteins such as BDLF-2. It has been shown that BMRF-2 and BDLF-2 form a complex and that BMRF-2 promotes the transport of BDLF-2 to the cell surface (Gore and Hutt-Fletcher, 2008). BDLF-2 also contains a potential tyrosine-containing YXXØ basolateral sorting signal in its C terminus, and the BMRF-2/BDLF-2 complex may accumulate in the TGN and subsequently be sorted to basolateral vesicles, facilitating delivery of nascent virions to the lateral membranes of epithelial cells. Thus, our data suggest that tyrosine- and dileucine-based basolateral sorting signals in the cytoplasmic tail of BMRF-2 may direct TGN/endosomal sorting vesicles containing nascent EBV virions to the basolateral membranes. Subsequently, virions released into the intercellular space interact with the integrins of neighboring cells via the BMRF-2 RGD domain, promoting direct cell-to-cell spread of virus from infected to uninfected cells.

Recently, it has been shown that the gamma-herpesvirus MHV-68 ORF58 and gp42 protein complex promote cell-to-cell spread of progeny virons by reorganizing the actin cytoskeleton and remodeling plasma membranes (Gill et al., 2008), leading to the formation of intercellular contacts. The role of gp42 was found to be critical in this process, whereas ORF58 was found to function in facilitating gp42 transport to the plasma membrane. EBV BDLF-2 and BMRF-2 are homologues of MHV-68 gp42 and ORF58, respectively. Gill at al. further showed that EBV BMRF-2/BDLF-1 may also induce this type of membrane remodeling (Gill et al., 2008). Accordingly, it is possible that EBV BDLF-2/BMRF-2 proteins use additional, alternative mechanisms to facilitate EBV spread that involve remodeling of plasma membranes, but this hypothesis remains to be tested in an EBV permissive model system.

In summary, in this study we provide the first evidence that, in addition to its contribution to initial viral infection from basolateral membranes, BMRF-2 may play an important role in facilitating the spread of EBV progeny virions through lateral membranes of polarized oral epithelial cells during productive infection. The tetrapeptide sequence YLLV in the cytoplasmic domain of BMRF-2 serves as a basolateral sorting signal for this protein, and BMRF-2 basolateral transport may serve as important determinant for distribution of progeny virions to the lateral membranes and their spread from infected to uninfected cells.

Materials and Methods

Cells and virus

To establish primary tongue and tonsil epithelial cell cultures, we used tissues from 2 tongues (TNG#1, TNG#2) and 3 tonsils (TNSL#1, TNSL#2, TNSL#3). Tongue biopsies were obtained from healthy volunteers, aged 32 and 41, using 5-mm– diameter biopsy punches (Department of Orofacial Sciences, UCSF). Tonsil tissues were purchased from the National Disease Research Interchange Program (Philadelphia, PA), from donors in the age range of 18 – 35 years. Primary keratinocytes from tongue and tonsil tissues were isolated and propagated according to published procedures (Maher et al., 2005; Pegtel, Middeldorp, and Thorley-Lawson, 2004), with some modifications. The 1–2 mm pieces of tongue and tonsil tissues were placed on Matrigel-coated plates and cultured in KGM-2 medium (Clonetics) at 37°C in a humidified incubator containing 5% CO_2. Approximately 2–3 weeks later, keratinocyte outgrowths formed around the tissue explants. They were then trypsinized, expanded as a primary culture in KGM-2 medium and frozen after passage 3 or 4. The epithelial origin of tongue and tonsil keratinocytes was confirmed by detection of pankeratins (using a cocktail of anti-keratin antibodies Ab-1 and Ab-2, Thermo Scientific). PCR analysis using EBV BZLF-1-specific primers (Xiao et al., 2008) showed that none of these cells contained EBV DNA, indicating that they were not infected with EBV in vivo.

Polarized cells were established in 12-mm–diameter, 0.45-μm pore size, polycarbonate membrane Transwell inserts (Costar Corp., Cambridge, Massachusetts), as described in our previous work (Tugizov, Maidji, and Pereira, 1996; Tugizov et al., 1998; Tugizov, Berline, and Palefsky, 2003). Development of epithelial cell polarity was confirmed by detection of the tight junction protein occludin and measurement of transepithelial resistance. Only fully polarized cells were used for the experiments.

The B95-8 EBV-producing marmoset B-lymphoblastoid cell line was maintained in RPMI 1640 medium, supplemented with 10% fetal calf serum. Recombinant EBV B27-BMRF-2^{low}, which expresses a low level of the BMRF-2 protein, was constructed in our laboratory by a homologous recombination method (Xiao et al., 2008). To disrupt expression of the BMRF-2 gene we used a PCR-generated DNA fragment containing green fluorescent protein (GFP) and neomycin/kanamycin (NK) resistance aminoglycoside phosphotransferase) expression cassettes, and infection of B lymphoblastoid cells and polarized oral epithelial cells with B27-BMRF-2^{low} virus was designed to generate a green signal. EBV replication was induced in B95-8 and B27- BMRF-2^{low} cells by adding 30 ng/ml 12-*O*-tetradecanoyl phorbol-13 acetate (PMA) and 4 mM butyric acid (both from Sigma) to the growth media for 10 days. Virus-containing media were cleared of cell debris by centrifugation at 5000 g for 15 min followed by filtration of the supernatant first through 0.8-μm pore-size filters and then through 0.45- μm pore-size filters (Millipore). Virus was then concentrated using Amicon Ultra-100 centrifugal filter devices (Millipore) and the viral titer was determined by quantitative real-time PCR as described in our previous work (Xiao et al., 2008; Xiao et al., 2007).

EBV cell-to-cell spread in polarized tongue and tonsil epithelial cells

To examine cell-to-cell spread of virus between polarized epithelial cells a viral plaque assay was used (Tugizov, Berline, and Palefsky, 2003). Cells were infected with B95-8 and B27-BMRF-2^{low} viruses at 0.3 virion/cell from the basolateral membrane. After 72 h, the culture medium was replaced with a medium containing a pool of EBV-neutralizing human sera at a dilution 1:100 in both the upper and lower chambers. This medium neutralizes released virions and therefore allows examination of cell-to-cell spread of viral progeny. The medium containing EBV-neutralizing human sera was replaced with fresh medium containing anti-EBV sera every 3–4 days until the experiment was completed. At 21 days post-infection, cells were fixed with 3% paraformaldehyde in PBS and immunostained with mAb against EBV gp350/220. Cells were analyzed by laser confocal microscopy using the Bio-Rad MRC2400. EBV spread was evaluated by quantitative analysis of foci or plaque formation (Tugizov, Berline, and Palefsky, 2003). Foci containing 5 or more infected cells were considered plaques. B95-8 -infected plaques were examined by gp350/220 immunostaining. B27-BMRF-2^{low} -infected plaques were analyzed by immunostaining of gp350/220 (red) and presence of a GFP signal that generated only by BMRF-2 knockout virus, and only those positive for both were accepted as B27-BMRF-2^{low} – generated plaques. The B27-BMRF-2^{low} virus generated plaques also were confirmed by immunostaining of cells with anti-BMRF-2 antibody, and negative BMRF-2 expression showed B27-BMRF-2^{low} -infected plaques.

Site-directed mutagenesis of the BMRF-2 protein and expression of the WT and mutant BMRF-2 proteins in HSC-3^{sort} cells

Cloning of the *BMRF-2* gene and expression of the BMRF-2 protein in HSC-3^{sort} cells were described previously (Xiao et al., 2007). Site-directed mutagenesis was performed to alter Y_{349}, and $LL_{350–351}$ using the QuikChange Site-Directed Mutagenesis Kit (Stratagene, San Diego, California) according to the protocols provided by the manufacturer. All mutagenic primers were synthesized by Invitrogen (Carlsbad, California). Primers for changing Y_{349} to A_{349}: bmrf2-349Y2A5 (forward primer) = 5’tttacttttgtgaagctctgttggtgacattc3’ and bmrf2-349Y2A3 (reverse primer) = aaatgtcaccaacagagcttcacaaaaagtaaag. Primers to replace $LL_{350–351}$ with $GG_{350–351}$:bmrf2-diLeu-m-5 (forward primer) = gtctttacttttgtgaatatggtggcgtgacattcattaaatc and bmrf2-diLeu-m-3 (reverse primer) = gatttaatgaatgtcacgccaccatattcacaaaaagtaaagac. Correct substitutions were confirmed by DNA sequencing and the BMRF-2 mutants were designated BMRF-$2_{Y\text{-}A}$ and BMRF-$2_{LL\text{-}GG}$ for substitution of Y_{349} and $LL_{350–351}$ respectively. BMRF-2 WT or mutant constructs tagged with green-fluorescent protein (GFP) were used to establish HSC-3^{sort} cell lines constitutively expressing BMRF-2 wt or mutant proteins by using ProPak A.52 retroviral expression system as described previously (Xiao et al., 2007). Clones expressing high levels of BMRF-2 were selected in growth medium containing Geneticin (G418, 500 μg/ml).

Western blot assay

Membrane protein extraction of HSC-3^{sort} cells expressing wt and mutant BMRF-2 proteins was performed as previously described (Xiao et al., 2007). Briefly, membrane fractions were solubilized in urea sample buffer (7 M urea, 2 M thioreurea, 1% TX100, 1% DTT, 4% chaps, and 10 mM Tris, pH 9.5) at room temperature for 1 h. Before loading, samples were mixed with one-tenth volume of 1 M DTT and denatured at 70 °C for 10 min. Proteins were then separated on 7 M urea-SDS PAGE gels and transferred to nitrocellulose membrane (Amersham). The BMRF-2 protein was detected using rat anti-BMRF-2 serum generated in our laboratory (Tugizov, Berline, and Palefsky, 2003) and the ECL detection kit (Roche).

Confocal immunofluorescence microscopy assay

For immunofluorescence assays cells were washed with phosphate-buffered saline (PBS, pH 7.2), fixed with 4% paraformaldehyde and 2% sucrose in PBS for 5 min, and then permeabilized with 0.01% Triton X-100 in 4% paraformaldehyde for 5 min. The EBV BMRF-2 and gp350/220 proteins were detected with rat anti-BMRF-2 serum (Tugizov, Berline, and Palefsky, 2003) and mouse anti-gp350/220 monoclonal antibodies (ABI), respectively.

For co-localization of BMRF-2 with markers of TGN46 and the μ subunit of AP-4, fixed and permeabilized infected cells were immunostained with mouse monoclonal antibodies (mAb) to TGN46 (Abcam Inc) and goat antibodies to AP-4μ (Santa Cruz, Biotech Inc). For co-localization of BMRF-2 with cadherin and integrin, cells were stained with rabbit antibodies to pan-cadherin (Abcam) and mAb's to β1 and αv integrin (Chemicon). BMRF-2 localization in the Golgi was examined by staining of BMRF-2-expressing polarized cells with Rhodamine-Lens Culinaris Agglutinin (Vector Laboratories). In these co-localization experiments BMRF-2 was detected by its GFP signal and the other proteins were revealed using the secondary antibodies conjugated to tetramethyl rhodamine isothiocyanate (TRITC) or Cy5, purchased from Jackson ImmunoResearch Laboratories (West Grove, Pennsylvania). In all immunostaining experiments, cell nuclei were counterstained with TO-PRO-3 (blue) (Molecular Probes).

Flow cytometry assays

Expression of wt and mutant BMRF-2 proteins on the cell surface of HSC-3^{sort} cell lines was determined by flow cytometry using rat anti–BMRF-2 serum (1:50). Cells were dissociated with enzyme-free cell dissociation buffer (Invitrogen), washed with cold PBS and incubated with primary antibodies in PBS containing 1% bovine serum albumin (BSA) for 1 h on ice. Cells were then washed in cold PBS and reacted with phycoerythrin-labeled goat–anti-rat antibodies for 30 min at 4°C. Cells were analyzed using a fluorescence-activated cell sorting (FACS) cytometer (Becton-Dickinson and Company, San Jose, California).

Domain-selective cell surface labeling assay

Polarized cells expressing wt and mutant BMRF-2 proteins were propagated in 24-mm–diameter, 0.45-μm pore size, polycarbonate membrane Transwell filters (Costar), and cells were labeled with 200 μg/ml sulfo-NHS-LC-biotin (Pierce) from apical or basolateral membranes for 30 min as described (Tugizov, Berline, and Palefsky, 2003). Cells were washed, cell extracts were made, and biotinylated proteins were precipitated with streptavidin-agarose beads Pierce), followed by separation on 7 M urea-SDS PAGE gel and transfer to nitrocellulose membranes (Amersham). The BMRF-2 protein was detected using rat anti-BMRF-2.

ACKNOWLEDGMENTS

We thank E. Lennette for providing EBV-neutralizing sera from nasopharyngeal carcinoma patients and M. Petitt for editorial assistance. This project was supported by NIH grants R01 DE14894 and R21 DE016009 (to ST).

References

Aguilar RC, Boehm M, Gorshkova I, Crouch RJ, Tomita K, Saito T, Ohno H, Bonifacino JS. Signal-binding specificity of the mu4 subunit of the adaptor protein complex AP-4. J Biol Chem 2001;276 (16):13145–13152. [PubMed: 11139587]

Alconada A, Bauer U, Baudoux L, Piette J, Hoflack B. Intracellular transport of the glycoproteins gE and gI of the varicella-zoster virus. gE accelerates the maturation of gI and determines its accumulation in the trans-Golgi network. J Biol Chem 1998;273(22):13430–13436. [PubMed: 9593675]

Alconada A, Bauer U, Hoflack B. A tyrosine-based motif and a casein kinase II phosphorylation site regulate the intracellular trafficking of the varicella-zoster virus glycoprotein I, a protein localized in the trans-Golgi network. Embo Journal 1996;15(22):6096–6110. [PubMed: 8947032]

Alconada AU, Bauler B, Sodiek B, Hoflack. Intracellular traffic of herpes simplex virus glycoprotein gE: Characterization of the sorting signals required for its trans-golgi network localization. Journal of virology 1998;73:377–387. [PubMed: 9847342]

Balan P, Davis PN, Bell S, Atkinson H, Browne H, Minson T. An analysis of the in vitro and in vivo phenotypes of mutants of herpes simplex virus type 1 lacking glycoproteins gG, gE, gI or the putative gJ. J Gen Virol 1994;75(Pt 6):1245–1258. [PubMed: 8207391]

Bonifacino JS, Marks MS, Ohno H, Kirchhausen T. Mechanisms of signal-mediated protein sorting in the endocytic and secretory pathways. Proc Assoc Am Physicians 1996;108(4):285–295. [PubMed: 8863342]

Bonifacino JS, Traub LM. Signals for sorting of transmembrane proteins to endosomes and lysosomes. Annu Rev Biochem 2003;72:395–447. [PubMed: 12651740]

Brack AR, Klupp BG, Granzow H, Tirabassi R, Enquist LW, Mettenleiter TC. Role of the cytoplasmic tail of pseudorabies virus glycoprotein E in virion formation. J Virol 2000;74(9):4004–4016. [PubMed: 10756012]

Browne H, Bell S, Minson T, Wilson DW. An endoplasmic reticulum-retained herpes simplex virus glycoprotein H is absent from secreted virions: evidence for reenvelopment during egress. J Virol 1996;70(7):4311–4316. [PubMed: 8676453]

Chang Y, Tung CH, Huang YT, Lu J, Chen JY, Tsai CH. Requirement for cell-to-cell contact in Epstein-Barr virus infection of nasopharyngeal carcinoma cells and keratinocytes. Journal of Virology 1999;73(10):8857–8866. [PubMed: 10482644]

Dell'Angelica EC, Mullins C, Bonifacino JS. AP-4, a novel protein complex related to clathrin adaptors. J Biol Chem 1999;274(11):7278–7285. [PubMed: 10066790]

Dingwell KS, Brunetti CR, Hendricks RL, Tang Q, Tang M, Rainbow AJ, Johnson DC. Herpes simplex virus glycoproteins E and I facilitate cell-to-cell spread in vivo and across junctions of cultured cells. J Virol 1994;68(2):834–845. [PubMed: 8289387]

Dingwell KS, Johnson DC. The herpes simplex virus gE-gI complex facilitates cell-to-cell spread and binds to components of cell junctions. J Virol 1998;72(11):8933–8942. [PubMed: 9765438]

Farnsworth A, Goldsmith K, Johnson DC. Herpes simplex virus glycoproteins gD and gE/gI serve essential but redundant functions during acquisition of the virion envelope in the cytoplasm. J Virol 2003;77(15):8481–8494. [PubMed: 12857917]

Farnsworth A, Johnson DC. Herpes simplex virus gE/gI must accumulate in the trans-Golgi network at early times and then redistribute to cell junctions to promote cell-cell spread. J Virol 2006;80(7):3167–3179. [PubMed: 16537585]

Farnsworth A, Wisner TW, Johnson DC. Cytoplasmic residues of herpes simplex virus glycoprotein gE required for secondary envelopment and binding of tegument proteins VP22 and UL11 to gE and gD. J Virol 2007;81(1):319–331. [PubMed: 17035313]

Feederle R, Neuhierl B, Bannert H, Geletneky K, Shannon-Lowe C, Delecluse HJ. Epstein-Barr virus B95.8 produced in 293 cells shows marked tropism for differentiated primary epithelial cells and reveals interindividual variation in susceptibility to viral infection. Int J Cancer 2007;121(3):588–594. [PubMed: 17417777]

Folsch H. The building blocks for basolateral vesicles in polarized epithelial cells. Trends Cell Biol 2005;15(4):222–228. [PubMed: 15817379]

Folsch H, Ohno H, Bonifacino JS, Mellman I. A novel clathrin adaptor complex mediates basolateral targeting in polarized epithelial cells. Cell 1999;99(2):189–198. [PubMed: 10535737]

Folsch H, Pypaert M, Maday S, Pelletier L, Mellman I. The AP-1A and AP-1B clathrin adaptor complexes define biochemically and functionally distinct membrane domains. J Cell Biol 2003;163(2):351–362. [PubMed: 14581457]

Folsch H, Pypaert M, Schu P, Mellman I. Distribution and function of AP-1 clathrin adaptor complexes in polarized epithelial cells. J Cell Biol 2001;152(3):595–606. [PubMed: 11157985]

Gershon AA, Sherman DL, Zhu Z, Gabel CA, Ambron RT, Gershon MD. Intracellular transport of newly synthesized varicella-zoster virus final envelopment in the trans-Golgi network. Journal of Virology 1994;68(10):6372–6390. [PubMed: 8083976]

Gill MB, Edgar R, May JS, Stevenson PG. A gamma-herpesvirus glycoprotein complex manipulates actin to promote viral spread. PLoS ONE 2008;3(3):e1808. [PubMed: 18350146]

Gore M, Hutt-Fletcher LM. The BDLF2 protein of Epstein-Barr virus is a type II glycosylated envelope protein whose processing is dependent on coexpression with the BMRF2 protein. Virology. 2008

Greenspan D, Greenspan JS. Oral manifestations of HIV infection. AIDS Clin Care 1997;9(4):29–33. [PubMed: 11364217]

Greenspan D, Greenspan JS, Hearst NG, Pan LZ, Conant MA, Abrams DI, Hollander H, Levy JA. Relation of oral hairy leukoplakia to infection with the human immunodeficiency virus and the risk of developing AIDS. J Infect Dis 1987;155(3):475–481. [PubMed: 3492574]

Greenspan JS, Greenspan D, Lennette ET, Abrams DI, Conant MA, Petersen V, Freese UK. Replication of Epstein-Barr virus within the epithelial cells of oral "hairy" leukoplakia, an AIDS-associated lesion. New England Journal of Medicine 1985;313(25):1564–1571. [PubMed: 2999595]

Henning W, Bohn W, Nebe B, Knopp A, Rychly J, Strauss M. Local increase of beta 1-integrin expression in cocultures of immortalized hepatocytes and sinusoidal endothelial cells. Eur J Cell Biol 1994;65 (1):189–199. [PubMed: 7534233]

Hunziker W, Harter C, Matter K, Mellman I. Basolateral sorting in MDCK cells requires a distinct cytoplasmic domain determinant. Cell 1991;66(5):907–920. [PubMed: 1909606]

Johnson DC, Huber MT. Directed egress of animal viruses promotes cell-to-cell spread. J Virol 2002;76 (1):1–8. [PubMed: 11739666]

Johnson DC, Webb M, Wisner TW, Brunetti C. Herpes simplex virus gE/gI sorts nascent virions to epithelial cell junctions, promoting virus spread. Journal of Virology 2001;75(2):821–33. [PubMed: 11134295]

Kieff, E.; Rickinson, A. "Epstein-Barr virus and its replication. In Fields Virology.". In: Knipe, DM.; Howley, PM., editors. Epstein-Barr virus and its replication. Vol. 4th edition. New York: Lippincott Williams and Willkins; 2001.

Lemon SM, Hutt LM, Shaw JE, Li JL, Pagano JS. Replication of EBV in epithelial cells during infectious mononucleosis. Nature 1977;268(5617):268–270. [PubMed: 196210]

Maher DM, Zhang ZQ, Schacker TW, Southern PJ. Ex vivo modeling of oral HIV transmission in human palatine tonsil. J Histochem Cytochem 2005;53(5):631–642. [PubMed: 15872056]

Marchisio PC, Bondanza S, Cremona O, Cancedda R, De Luca M. Polarized expression of integrin receptors (alpha 6 beta 4, alpha 2 beta 1, alpha 3 beta 1, and alpha v beta 5) and their relationship with the cytoskeleton and basement membrane matrix in cultured human keratinocytes. J Cell Biol 1991;112(4):761–773. [PubMed: 1825212]

May JS, de Lima BD, Colaco S, Stevenson PG. Intercellular gamma-herpesvirus dissemination involves co-ordinated intracellular membrane protein transport. Traffic 2005a;6(9):780–793. [PubMed: 16101681]

May JS, Walker J, Colaco S, Stevenson PG. The murine gammaherpesvirus 68 ORF27 gene product contributes to intercellular viral spread. J Virol 2005b;79(8):5059–5068. [PubMed: 15795291]

McMillan TN, Johnson DC. Cytoplasmic domain of herpes simplex virus gE causes accumulation in the trans-Golgi network, a site of virus envelopment and sorting of virions to cell junctions. J Virol 2001;75(4):1928–1940. [PubMed: 11160692]

Niedobitek G, Young LS, Lau R, Brooks L, Greenspan D, Greenspan JS, Rickinson AB. Epstein-Barr virus infection in oral hairy leukoplakia: virus replication in the absence of a detectable latent phase. J Gen Virol 1991;72(Pt 12):3035–3046. [PubMed: 1662695]

Ohno H, Stewart J, Bosshart H, Rhee I, Miyatake S, Saito T, Gallusser A, Kirchhausen T, Bonifacino JS. Interaction of tyrosine-based sorting signals with clathrin-associated proteins. Science 1995;269 (5232):1872–1075. [PubMed: 7569928]

Ohno H, Tomemori T, Nakatsu F, Okazaki Y, Aguilar RC, Foelsch H, Mellman I, Saito T, Shirasawa T, Bonifacino JS. Mu1B, a novel adaptor medium chain expressed in polarized epithelial cells. FEBS Lett 1999;449(2–3):215–220. [PubMed: 10338135]

Pegtel DM, Middeldorp J, Thorley-Lawson DA. Epstein-Barr virus infection in ex vivo tonsil epithelial cell cultures of asymptomatic carriers. J Virol 2004;78(22):12613–12624. [PubMed: 15507648]

Philp NJ, Nachmias VT. Polarized distribution of integrin and fibronectin in retinal pigment epithelium. Invest Ophthalmol Vis Sci 1987;28(8):1275–1280. [PubMed: 3301730]

Polcicova K, Goldsmith K, Rainish BL, Wisner TW, Johnson DC. The extracellular domain of herpes simplex virus gE is indispensable for efficientcell-to-cell spread: evidence for gE/gI receptors. J Virol 2005;79(18):11990–12001. [PubMed: 16140775]

Rajasekaran AK, Humphrey JS, Wagner M, Miesenbock G, Le Bivic A, Bonifacino JS, Rodriguez-Boulan E. TGN38 recycles basolaterally in polarized Madin-Darby canine kidney cells. Mol Biol Cell 1994;5(10):1093–1103. [PubMed: 7865877]

Renold A, Cescato R, Beuret N, Vogel LK, Wahlberg JM, Brown JL, Fiedler K, Spiess M. Basolateral sorting signals differ in their ability to redirect apical proteins to the basolateral cell surface. J Biol Chem 2000;275(13):9290–9295. [PubMed: 10734069]

Rickinson A. Epstein-Barr virus in epithelium. Nature 1984;310(5973):99–100. [PubMed: 6330572]

Rickinson, A.; Kieff, E. "Epstein-Barr Virus. In Fields Virology.". In: Fields, BN.; Knipe, DM.; Howley, PM., editors. Epstein-Barr Virus. Vol. Vol. 2. Philadelphia: Lippincott-Williams and Wilkins; 2001.

Sattentau Q. Avoiding the void: cell-to-cell spread of human viruses. Nat Rev Microbiol 2008;6(11): 815–826. [PubMed: 18923409]

Sevier CS, Weisz OA, Davis M, Machamer CE. Efficient export of the vesicular stomatitis virus G protein from the endoplasmic reticulum requires a signal in the cytoplasmic tail that includes both tyrosine-based and di-acidic motifs. Mol Biol Cell 2000;11(1):13–22. [PubMed: 10637287]

Simmen T, Honing S, Icking A, Tikkanen R, Hunziker W. AP-4 binds basolateral signals and participates in basolateral sorting in epithelial MDCK cells. Nat Cell Biol 2002;21:21.

Sixbey JW, Nedrud JG, Raab-Traub N, Hanes RA, Pagano JS. Epstein-Barr virus replication in oropharyngeal epithelial cells. New England Journal of Medicine 1984;310(19):1225–1230. [PubMed: 6323983]

Sixbey JW, Vesterinen EH, Nedrud JG, Raab-Traub N, Walton LA, Pagano JS. Replication of Epstein-Barr virus in human epithelial cells infected in vitro. Nature 1983;306(5942):480–483. [PubMed: 6316160]

Skepper JN, Whiteley A, Browne H, Minson A. Herpes simplex virus nucleocapsids mature to progeny virions by an envelopment --> deenvelopment --> reenvelopment pathway. J Virol 2001;75(12): 5697–5702. [PubMed: 11356979]

Tirabassi RS, Enquist LW. Role of envelope protein gE endocytosis in the pseudorabies virus life cycle. J Virol 1998;72(6):4571–4579. [PubMed: 9573220]

Tirabassi RS, Enquist LW. Mutation of the YXXL endocytosis motif in the cytoplasmic tail of pseudorabies virus gE. J Virol 1999;73(4):2717–2728. [PubMed: 10074118]

Tugizov S, Herrera R, Veluppillai P, Greenspan J, Greenspan D, Palefsky JM. Epstein-Barr Virus (EBV)-Infected Monocytes Facilitate Dissemination of EBV within the Oral Mucosal Epithelium. J Virol 2007;81(11):5484–5496. [PubMed: 17376918]

Tugizov S, Maidji E, Pereira L. Role of apical and basolateral membranes in replication of human cytomegalovirus in polarized retinal pigment epithelial cells. J Gen Virol 1996;77(Pt 1):61–74. [PubMed: 8558129]

Tugizov S, Maidji E, Xiao J, Zheng Z, Pereira L. Human cytomegalovirus glycoprotein B contains autonomous determinants for vectorial targeting to apical membranes of polarized epithelial cells. J. Virol 1998;72:7374–7386. [PubMed: 9696834]

Tugizov SM, Berline JW, Palefsky JM. Epstein-Barr virus infection of polarized tongue and nasopharyngeal epithelial cells. Nat Med 2003;9(3):307–314. [PubMed: 12592401]

Turcotte S, Letellier J, Lippe R. Herpes simplex virus type 1 capsids transit by the trans-Golgi network, where viral glycoproteins accumulate independently of capsid egress. J Virol 2005;79(14):8847–8860. [PubMed: 15994778]

Whiteley A, Bruun B, Minson T, Browne H. Effects of targeting herpes simplex virus type 1 gD to the endoplasmic reticulum and trans-Golgi network. J Virol 1999;73(11):9515–9520. [PubMed: 10516060]

Xiao J, Palefsky JM, Herrera R, Berline J, Tugizov SM. The Epstein-Barr virus BMRF-2 protein facilitates virus attachment to oral epithelial cells. Virology 2008;370(2):430–442. [PubMed: 17945327]

Xiao J, Palefsky JM, Herrera R, Tugizov SM. Characterization of the Epstein-Barr virus glycoprotein BMRF-2. Virology 2007;359(2):382–396. [PubMed: 17081581]

Young LS, Dawson CW, Clark D, Rupani H, Busson P, Tursz T, Johnson A, Rickinson AB. Epstein-Barr virus gene expression in nasopharyngeal carcinoma. J Gen Virol 1988;69(Pt 5):1051–1065. [PubMed: 2836550]

Zhu Z, Hao Y, Gershon MD, Ambron RT, Gershon AA. Targeting of glycoprotein I (gE) of varicella-zoster virus to the trans-Golgi network by an AYRV sequence and an acidic amino acid-rich patch in the cytosolic domain of the molecule. Journal of Virology 1996;70(10):6563–6575. [PubMed: 8794291]

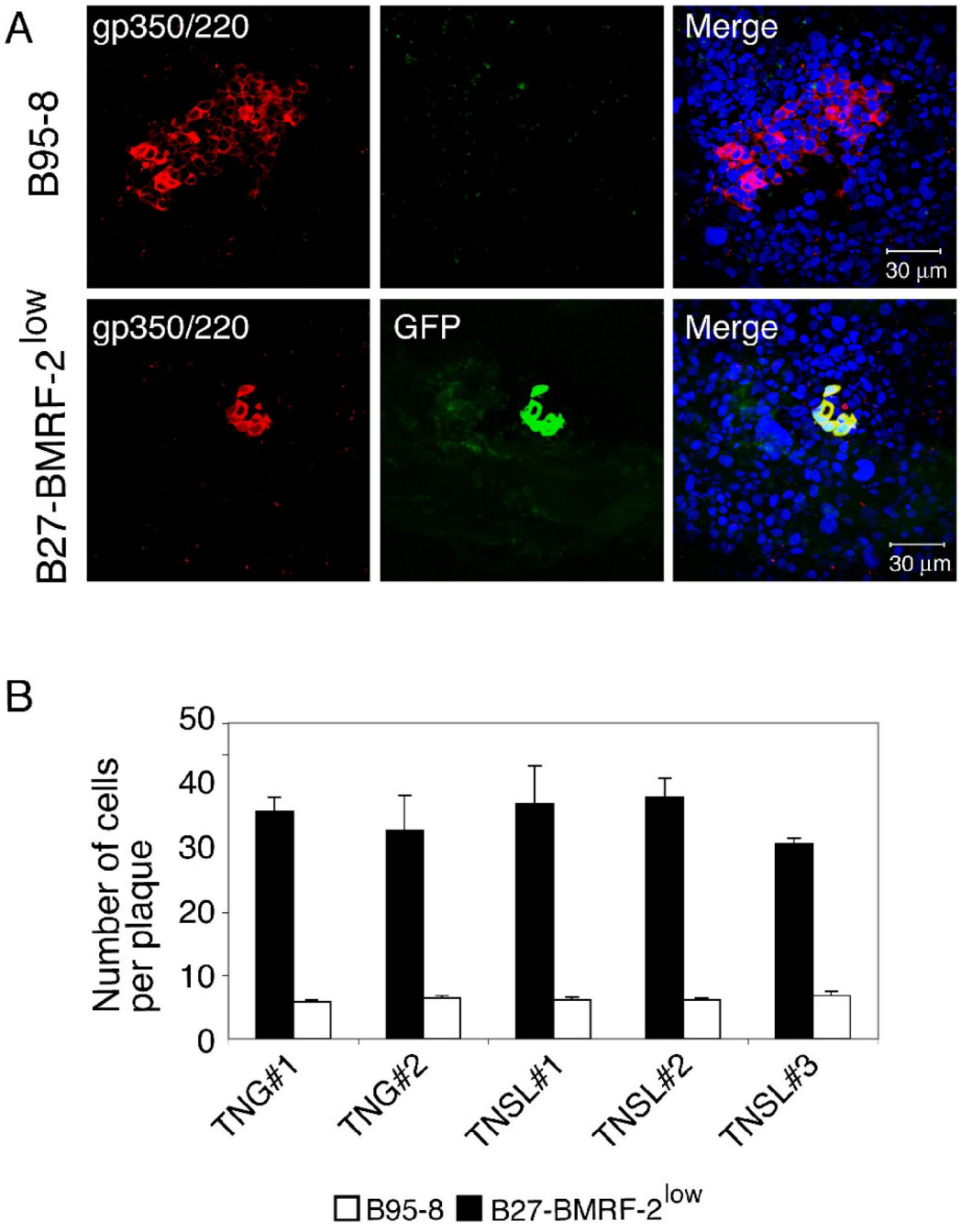

Fig. 1.

Cell-to-cell spread of B95-8 and B27-BMRF-2^{low} virus within the polarized tongue and tonsil epithelial cells. (A) Polarized tongue TNG#1 cells were infected with B95-8 (upper panels) or B27-BMRF-2^{low} virus (lower panel), and after 3 weeks they were fixed and immunostained using anti-gp350/250 antibodies (red). Green in the lower panels indicates GFP expression by the BMRF-2 knockout virus. Yellow in the merged lower panel represents colocalization of GFP and gp350/220. Nuclei were counterstained in blue. (B) Polarized tongue and tonsil cells were infected with B95-8 or B27-BMRF-2^{low} viruses, and after 3 weeks cells were analyzed for virus spread. Cell-to-cell spread of viruses was quantitatively evaluated by counting of EBV-infected cells in B95-8- and B27-BMRF-2^{low}- infected plaques. EBV B95-8-infected

plaques were detected by gp350/220-positive cells. B27-BMRF-2^{low} -infected plaques were identified by co-localization of the GFP signal with gp350/220. Results are represented as the average number of EBV-infected cells per plaque. Error bars indicate s.e.m. (n=5). Similar results were obtained in three independent experiments.

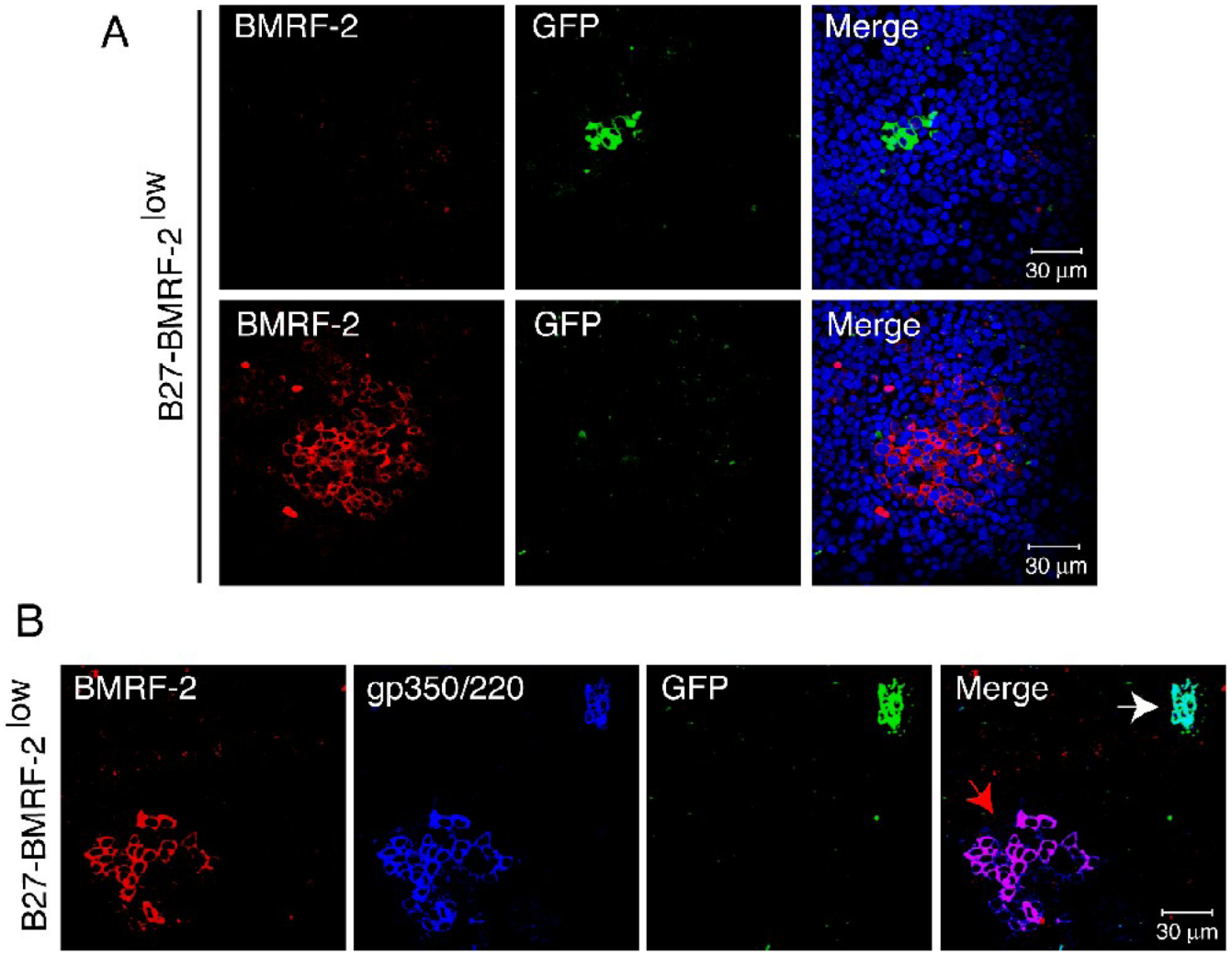

Fig. 2.

Analysis of cell-to-cell spread of B27-BMRF-2^{low} virus. Polarized tongue epithelial cells (TNG#1) were infected with B27-BMRF-2^{low} virus from their basolateral membranes, and after 3 weeks, cells were fixed and analyzed for plaque development. (A) Cells were immunostained with rat anti-BMRF-2 antibody (red). Cell nuclei were counterstained in blue. Green in upper panels indicates B27-BMRF-2^{low} virus infected cells. (B) Cells were immunostained with rat anti-BMRF-2 (red) and mouse antigp350/220 (blue) antibodies. Green GFP signal indicates B27-BMRF-2^{low} virus infected cells. White arrow shows BMRF-2–negative, gp350-positive and GFP-positive small plaque. Red arrow shows a BMRF-2–positive, gp350-positive and GFP-negative large plaque.

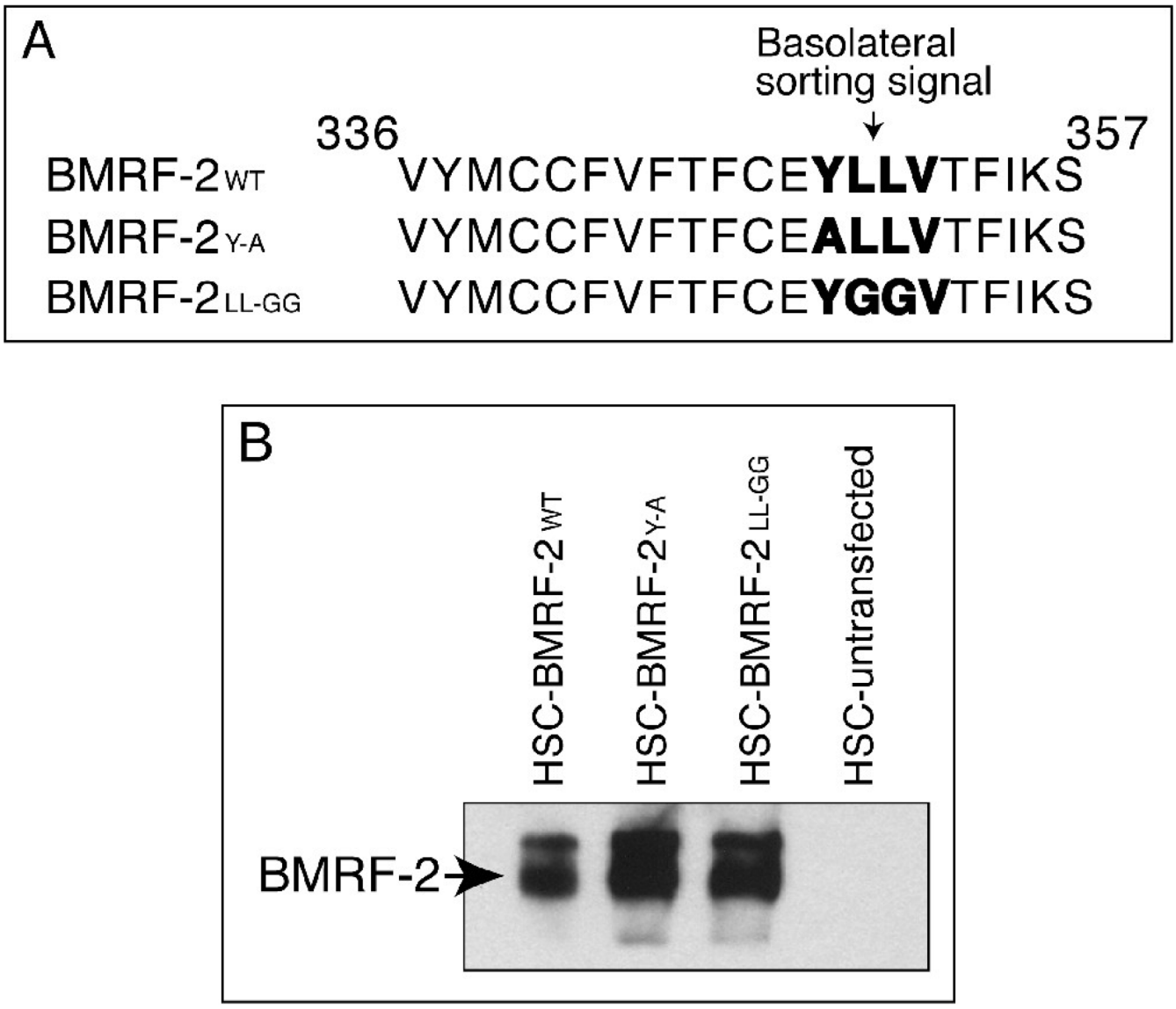

Fig. 3.

Expression of the wt BMRF-2 and its tyrosine and di-leucine mutants in oral epithelial cells. (A) Site-specific mutagenesis of the BMRF-2 cytoplasmic sorting motif YLLV (in bold) with substitution of tyrosine$_{349}$ with alanine (BMRF-2$_{Y\text{-}A}$) and the di-leucine$_{350–351}$ with glycines (BMRF-2 $_{LL\text{-}GG}$. (B) Western blot analysis of wt and mutant BMRF-2 proteins in HSC-BMRF-2$_{wt}$, HSC-BMRF-2$_{Y\text{-}A}$ and HSC-BMRF-2$_{LL\text{-}GG}$ cells. Membrane fractions were separated on urea-SDS PAGE gels and transferred to nitrocellulose membranes. BMRF-2 protein was detected using rat anti-BMRF-2 serum.

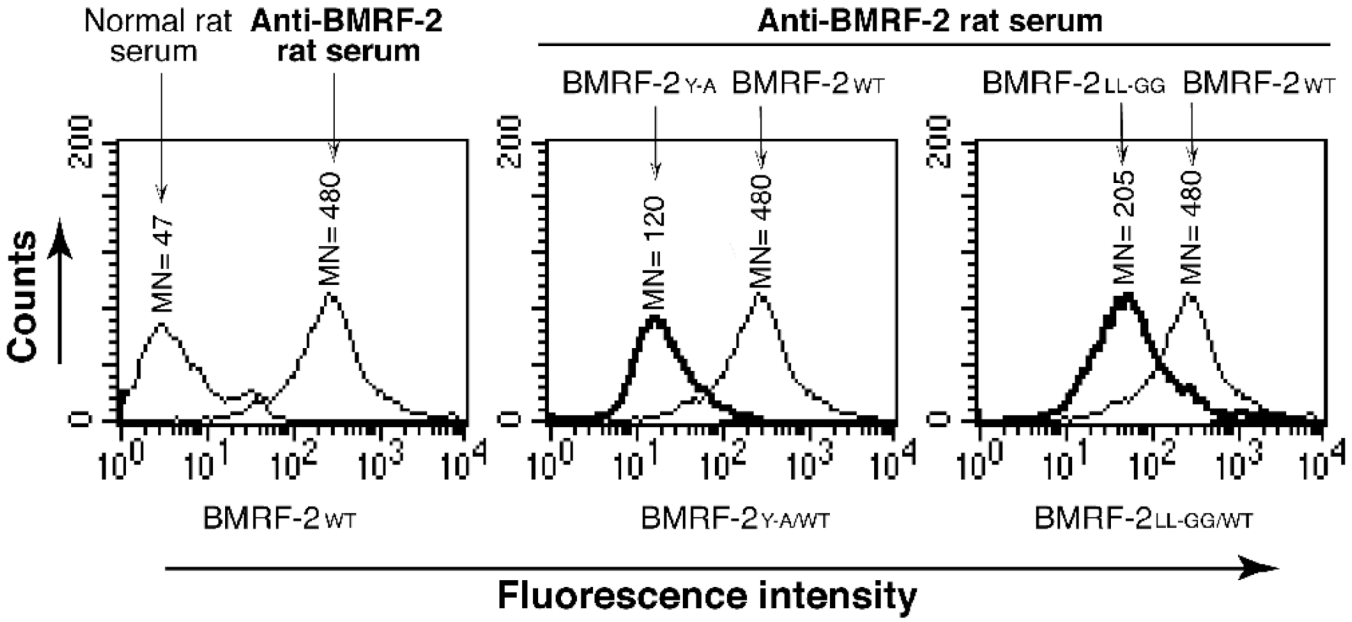

Fig. 4.

Flow cytometry analysis of cell surface expression of wt and mutant BMRF-2 proteins in non-polarized HSC-3 oral epithelial cells. HSC-BMRF-2_{wt}, HSC-BMRF-$2_{Y\text{-}A}$ and HSC-BMRF-$2_{LL\text{-}GG}$ cell lines expressing wt BMRF-2 and its tyrosine and dileucine mutants were grown under non-polarizing conditions and dissociated with enzyme-free cell-dissociation buffer. Expression of BMRF-2 on the cell surface was examined by flow cytometry in HSC-BMRF-2_{wt} (left panel), HSC-BMRF-$2_{Y\text{-}A}$ (middle panel), and HSC-BMRF-$2_{LL\text{-}GG}$ (right panel) cell lines using rat anti-BMRF-2 serum. Surface expression of BMRF-$2_{Y\text{-}A}$ and BMRF-$2_{LL\text{-}GG}$ mutant proteins were compared with wt BMRF-2 by superimposing the histograms for the HSC-BMRF-$2_{Y\text{-}A}$ and HSC-BMRF-$2_{LL\text{-}GG}$ cell lines on the histogram for HSC-BMRF-2_{wt} cells. MN, mean fluorescence intensity.

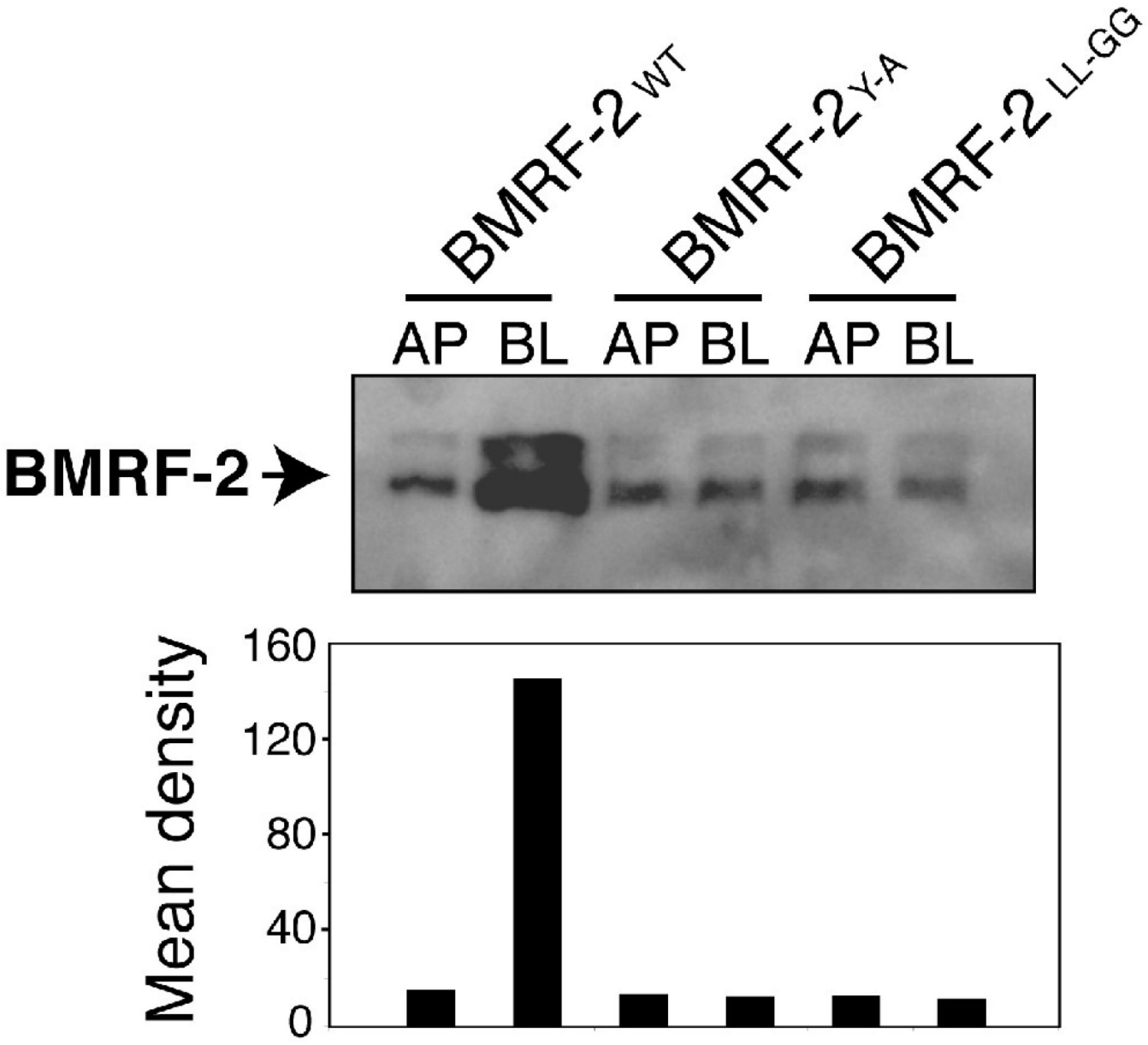

Fig. 5.

Analysis of BMRF-2 protein on the surface of polarized cells using a domain-selective surface labeling assay. HSC-BMRF-2_{wt}, HSC-BMRF-$2_{Y\text{-}A}$ and HSC-BMRF-$2_{LL\text{-}GG}$ cell lines were grown under polarized conditions and their apical or basolateral surfaces were independently labeled with sulfo-NHS-LC-biotin. Cells extracts were made, biotinylated proteins were precipitated with streptavidin-agarose beads and equal amounts of total protein were separated by urea-SDS PAGE gel electrophoresis. BMRF-2 protein was detected using rat anti-BMRF-2 serum. The amounts of wt and mutant BMRF-2 proteins were measured by determining the mean pixel densities of the protein bands, as indicated in the bar graphs under each protein.

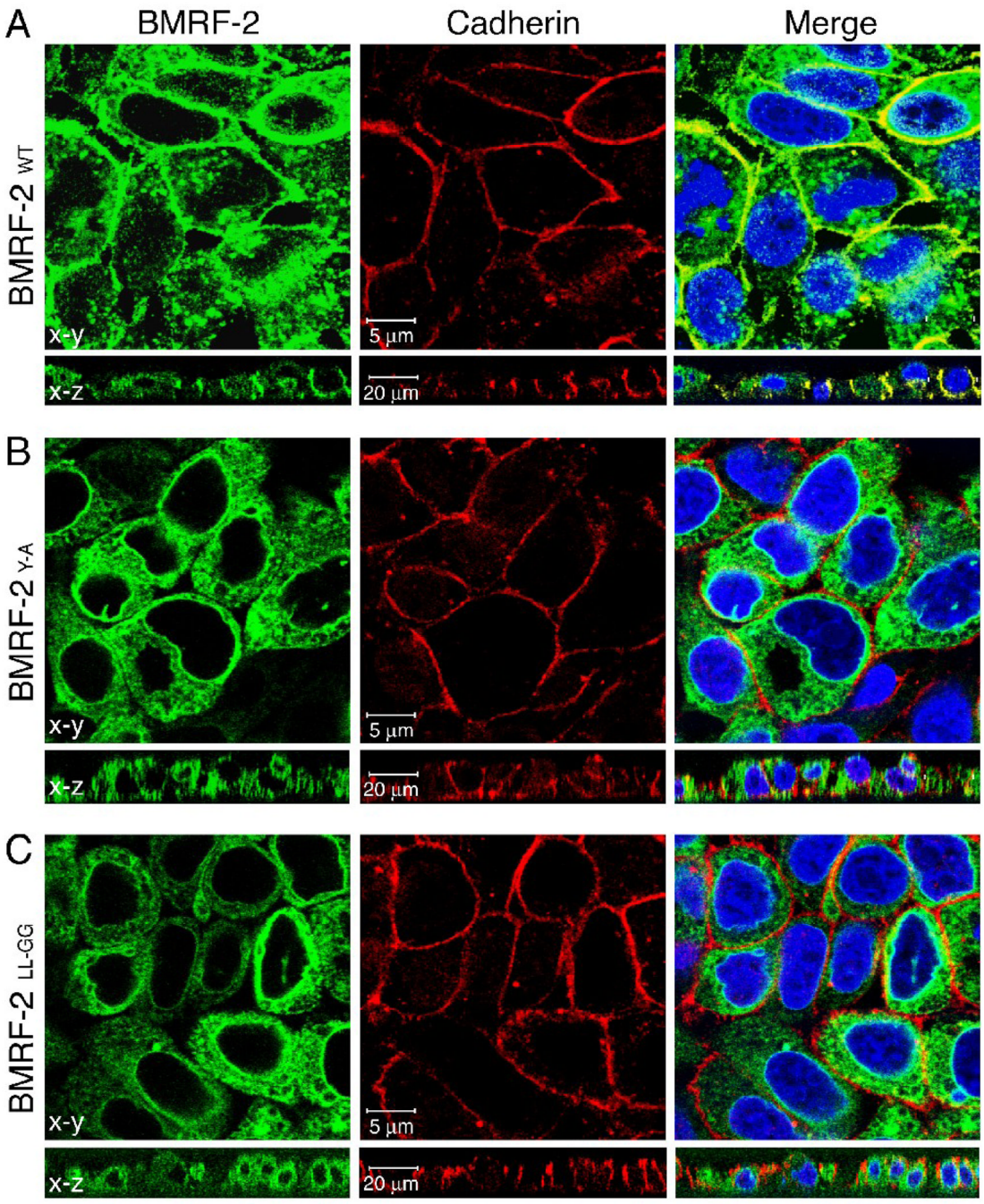

Fig. 6.

Confocal microscopy analysis of basolateral membrane transport of the wt and mutant BMRF-2 proteins. Polarized HSC-BMRF-2_{wt}(A), HSC-BMRF-$2_{Y\text{-}A}$ (B) and HSCBMRF- $2_{LL\text{-}GG}$ (C) cell lines were immunostained for pan-cadherin and analyzed by confocal microscopy by x-y horizontal and x-z vertical planes. Nuclei were counterstained in blue. Yellow in the merged panel indicates colocalization of BMRF-2– GFP (green) and pan-cadherin (red) on the basolateral cell surface.

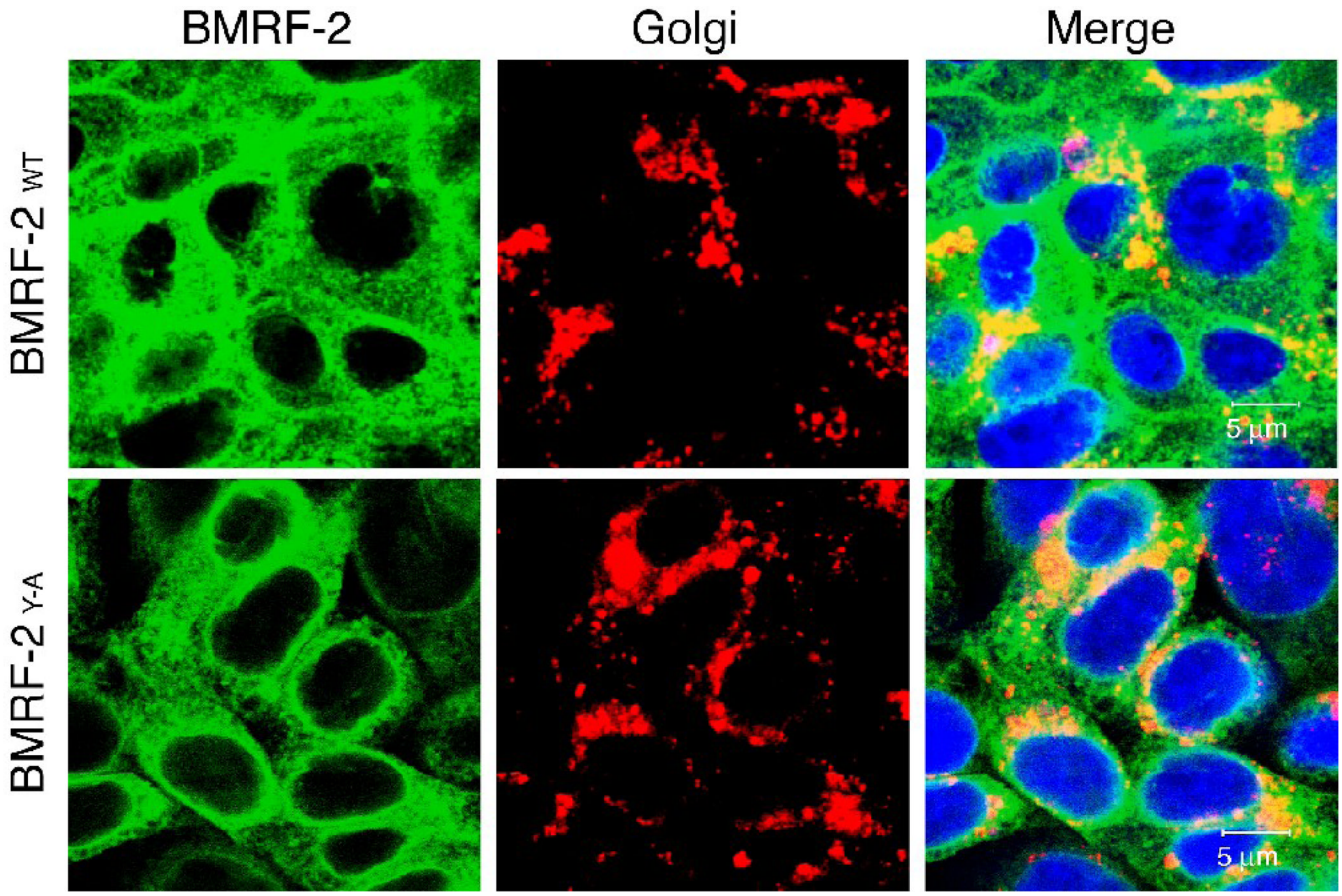

Fig. 7.

Localization of wt and mutant BMRF-2 proteins in the Golgi compartment. Polarized HSC-BMRF-2_{wt} and HSC-BMRF-$2_{Y\text{-}A}$ cell lines were fixed and stained with the Golgi marker Rhodamine-Lens Culinaris Agglutinin. BMRF-2 is shown in green fluorescence from a GFP fusion protein, and the Golgi marker is shown in red. Yellow indicates colocalization of BMRF-2 with the Golgi marker.

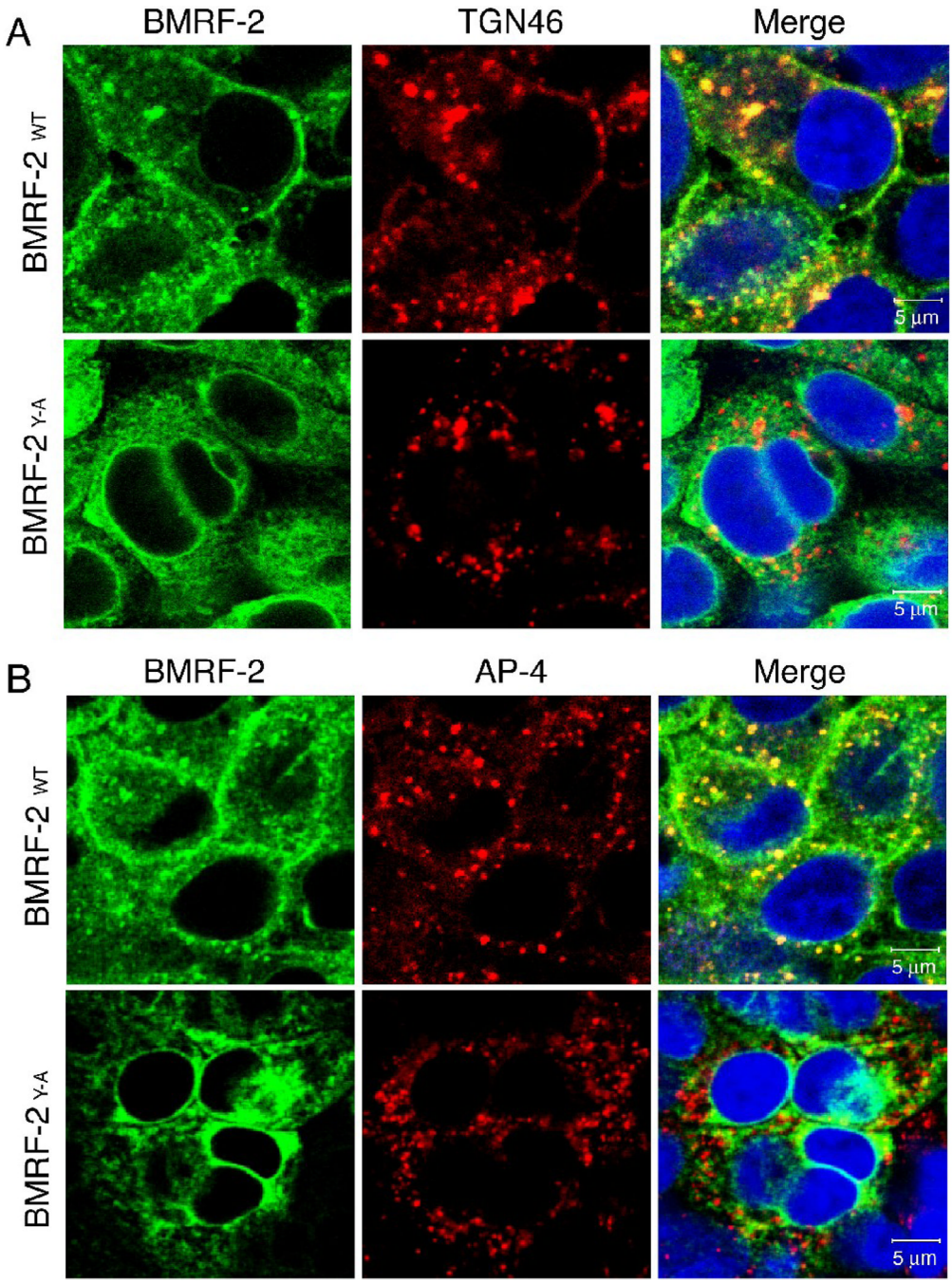

Fig. 8.

Accumulation of BMRF-2 in the TGN and in the basolateral sorting vesicles of polarized HSC-3 cells. Polarized HSC-BMRF-2_{wt} and HSC-BMRF-$2_{Y\text{-}A}$ cell lines were immunostained for TGN46 (A) and AP4μ (B), and colocalization of wt and mutant BMRF-2 proteins with TGN46 and AP-4μ was examined by confocal microscopy. Yellow in the merged panel indicates colocalization of BMRF-2-GFP (green) and TGN46 or AP4μ (red) proteins. Cell nuclei were counterstained in blue.

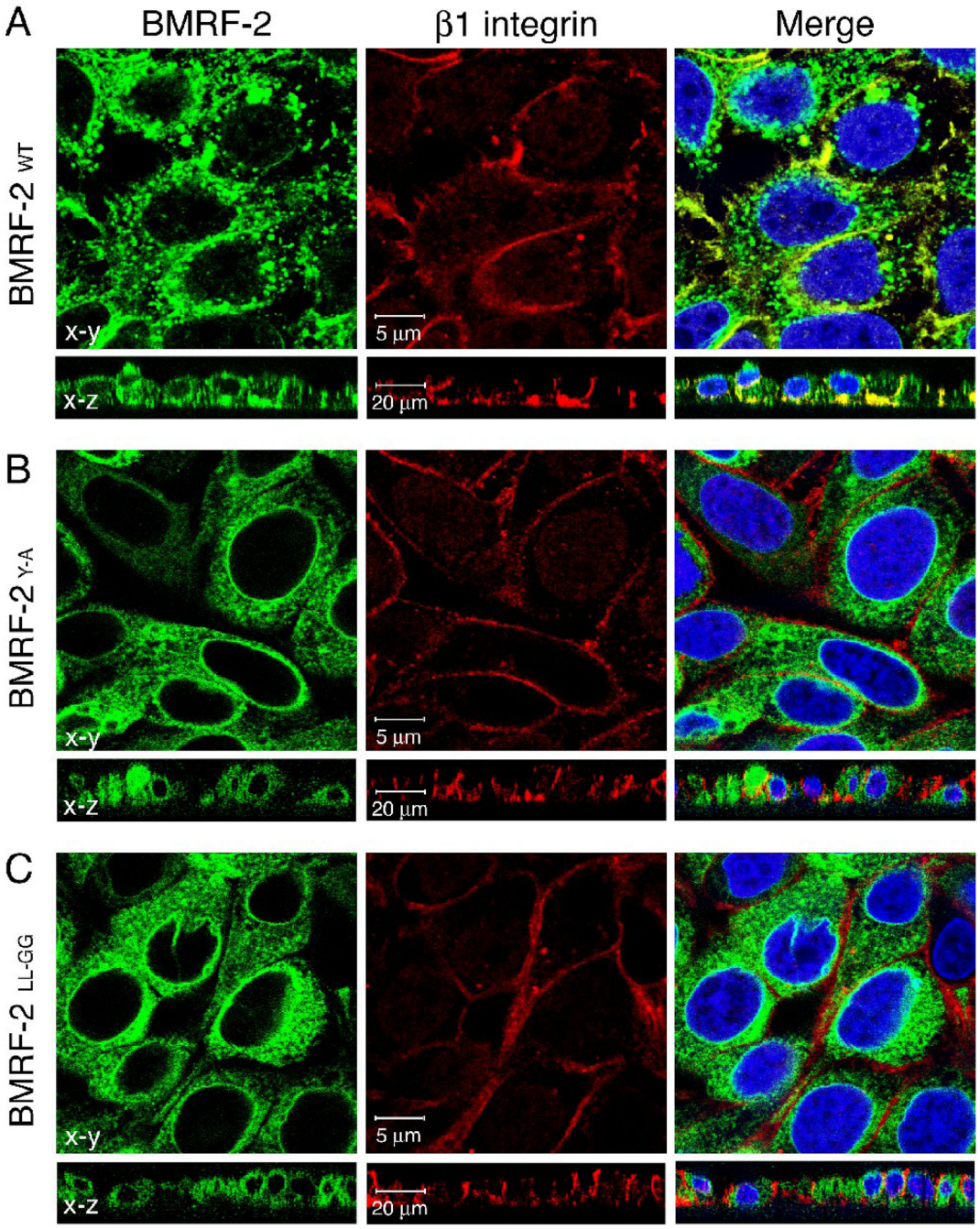

Fig. 9.

Confocal microscopy analysis of BMRF-2 interaction with β1 integrin in polarized oral epithelial cells. Polarized HSC-BMRF-2_{wt} (A), HSC-BMRF-$2_{Y\text{-}A}$ (B) and HSC-BMRF-$2_{LL\text{-}GG}$ (C) cells were immunostained for β1 integrin and then examined by confocal microscopy. Images were obtained in both x-y horizontal and x-z vertical planes. Yellow in the merged panel indicates colocalization of BMRF-2–GFP (green) and β integrin (red). Cell nuclei were counterstained in blue.